



# INTERNATIONAL JOURNAL OF PURE AND APPLIED RESEARCH IN ENGINEERING AND TECHNOLOGY

A PATH FOR HORIZING YOUR INNOVATIVE WORK



## SPECIAL ISSUE FOR INTERNATIONAL LEVEL CONFERENCE "ADVANCES IN SCIENCE, TECHNOLOGY & MANAGEMENT" (IC-ASTM)

### X- RAY DIFFRACTION STUDY OF DRAGLINE SILK OF NEPHILA PILIPES (ARANEAE; ARANEIDAE)

A. S. SAWARKAR , S. B. SAWARKAR

1. Department of Zoology, Shri R. L. T. College of Science, Akola 444001
2. Department of Physics, Shri Shivaji College of Arts, Commerce & Science, Akola 444001

Accepted Date: 05/09/2017; Published Date: 10/10/2017

**Abstract:** Orb web spider *Nephila pilipes* produces six different types of silks like dragline, auxiliary spiral, egg sac silk, sticky capture silk, attachment discs, swathing bands etc. The x- ray diffraction pattern of dragline silk of *Nephila pilipes* was recorded. The dragline silk of *Nephila pilipes* showed very broad x- ray diffractogram at  $2\theta = 10^\circ - 40^\circ$ . The x- ray diffraction patterns are composed of two phases called as amorphous and crystalline. Spider silk has semicrystalline structure with crystalline particles embedded in the amorphous matrix. In dragline silk, particle size ranges from 0.99 – 4.37 nm. Average crystallite size of dragline silk was found to be 2.1 nm. In *Nephila pilipes*, protein crystals occupy 44.97 % of total volume of dragline silk. Remaining volume of silk is amorphous in nature. This nanostructural features of spider silk plays very important role in enhancing mechanical performance of silk threads. Hence, it can be concluded that, spider silk having high and stable mechanical performance is found in nature. Successful large scale production of this beautiful, naturally golden colored spider silk with DNA recombinant technology will definitely open a new gate in textile sector.

**Keywords:** Dragline silk, *Nephila pilipes*, x- ray diffraction.

Corresponding Author: MR. A. S. SAWARKAR

Co Author: - MR. S. B. SAWARKAR

Access Online On:

[www.ijpret.com](http://www.ijpret.com)

How to Cite This Article:

A. S. Sawarkar, IJPRET, 2017; Volume 6 (2): 66-69



PAPER-QR CODE

## INTRODUCTION

The study of properties of spider silk is very important as it contributes significantly to the understanding of spider wealth. Spider silk is known for its outstanding properties. Various kinds of silk producing glands in spider function as small biofactories. The secretion of each gland performs definite function. Yellowish golden colored dragline silk is produced by a pair of ampullate glands of *Nephila pilipes*. Silk appears in variety of physico-chemical forms from the body of this single individual. Kennedy *et al.* (2005) presented x- ray diffraction as an effective and sensitive method of analyzing the condition of silk. Trancik *et al.* (2006) used Transmission Electron Microscopy and x- ray diffraction to examine the nanostructure of spider dragline silk from cob web weaving spider, *Latrodectus hesperus*. To plentifully benefit from its properties (mechanical, optical, biological) and its potential to manufacture green materials, the structure of spider silk has to be known accurately (Dionne, *et al.*, 2016). To this aim, x- ray diffraction study was used for structural characterization of dragline silk of *Nephila pilipes*.

## MATERIAL AND METHODS

Dragline silk samples were taken from the frame threads of the orb web of female *Nephila pilipes*. A bundle of 15-20 individual dragline fiber was held taut but unstretched on a glass slide, with the fiber axis normal to the X- ray beam. The x- ray diffraction patterns of dragline silk was recorded on Rigaku x-ray diffractometer, Miniplex II with nickel filtered  $\text{CuK}\alpha$  radiation ( $\lambda = 1.5406 \text{ \AA}$ ) in scanning angle range of  $10^\circ - 50^\circ$ . Microcal Origin was used for deconvolution of x-ray data and peak fitting. The **crystallinity index** was calculated as –

$$X_c = \frac{A_c}{A_c + A_a} \times 100 \%$$

Where,  $X_c$  = Percentage crystallinity,  $A_c$  = Area of crystalline portion and  $A_c + A_a$  = Total area of amorphous and crystalline portion of x- ray diffractogram.

Average **crystallite size** was determined using Scherer's formula by choosing all possible convenient peaks after 51 point smoothing of original diffractogram as –

$$\text{Crystallite Size (D)} = \frac{\lambda k}{\beta \cos \theta}$$

Where,  $\lambda$  = x- ray wavelength ( $1.5406 \text{ \AA}$ ),  $k$  = Shape factor for crystallite (0.94),  $\beta$  = Full width at half maximum (FWHM) in radian and  $\theta$  = Scanning angle in degree.

## RESULTS AND DISCUSSIONS

The natural dragline silk of *Nephila pilipes* showed very broad x- ray diffractogram at  $2\theta = 10^\circ - 40^\circ$ . Fig. 1 displayed typical well fitted peaks after 51 point smoothing of the original pattern. X-ray diffraction analysis of bundle of silk threads has shown that spider silk is composed of both crystalline and amorphous fraction. (Grubb and Jelinski, 1997; Riekel *et al.*, 1999). In *Nephila pilipes*, protein crystals occupy 44.97 % of total volume of dragline silk. Remaining volume of silk is amorphous in nature i.e. contains protein chains. Silk has semicrystalline structure with crystalline particles embedded in the amorphous matrix. The Semicrystalline nature of dragline silk of *Nephila pilipes* was also confirmed with the help of AFM images and FTIR spectrum (Sawarkar, 2016). In dragline silk, particle size ranges from 0.99 – 4.37 nm and average crystallite size was found to be 2.1 nm (Table 1).

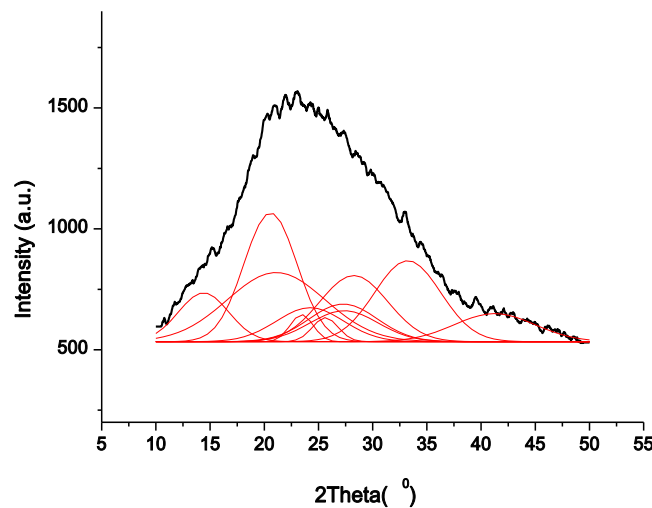


Fig. 1: X-ray diffraction pattern of dragline silk of *Nephila pilipes* after 51 point smoothing.

Table 1: Average crystallite size of dragline silk

Scanning angle ( $2\theta^\circ$ )	$\theta^\circ$	$\theta$ (rad)	FWHM ( $\beta$ )	$\beta$ (rad)	$\cos \theta$ (rad)	X-ray wavelength ( $\lambda$ )	Crystallite Size (D) nm
14.398	7.199	0.125579	4.6515	0.081141	0.992125	1.540598	1.913743
20.569	10.2845	0.179403	4.8823	0.085167	0.98395	1.540598	1.838424
21.1	10.55	0.184034	9.0146	0.157251	0.983113	1.540598	0.996536
24.227	12.1135	0.211308	6.2057	0.108252	0.977757	1.540598	1.455531
27.289	13.6445	0.238015	6.2715	0.1094	0.971808	1.540598	1.449077
33.231	16.6155	0.289841	6.0981	0.106375	0.958289	1.540598	1.511305
41.253	20.6265	0.359809	7.4429	0.129834	0.935964	1.540598	1.267774
28.261	14.1305	0.246492	6.2622	0.109238	0.969774	1.540598	1.454272
28.261	14.1305	0.246492	6.2622	0.109238	0.969774	1.540598	1.454272
27.368	13.684	0.238704	6.2752	0.109465	0.971645	1.540598	1.448465
23.444	11.722	0.204479	2.1295	0.037147	0.979167	1.540598	4.235541
25.633	12.8165	0.223571	2.364	0.041238	0.975112	1.540598	3.831257
42.486	21.243	0.370563	2.1656	0.037777	0.932124	1.540598	4.375135
Average							2.094718

Sampath *et al.* (2012) calculated 28 % crystallinity in major ampullate gland silk of *Nephila clavipes* and 31 % in major ampullate gland silk of *Argiope aurantia*. They also found crystallite size in the range of 2-10 nm. A smaller crystallite size means a smaller number of defects in the crystallite. Therefore, the reduced size of crystallite could be another contributor to the improvement of the breaking stress and the yield stress (Du *et al.*, 2006). Thus, enhancement of spider silk strength can be achieved by decreasing crystallite size. Keten *et al.* (2010) reported a series of large scale molecular dynamics simulations, revealing that  $\beta$ -sheet nanocrystals confined to a few nanometers achieve higher stiffness, strength and mechanical toughness than larger nanocrystals. Their findings explained how size effects can be exploited to create bioinspired materials with superior mechanical properties. Papadopoulos *et al.* (2007) employed polarized Fourier Transform Infrared (FTIR) spectroscopy to study structure-

property relationship in major ampullate spider silk being exposed to an external mechanical strain. They found that alanine rich  $\beta$ -sheeted crystals are oriented along the silk fiber axis and are interlinked by glycine-rich chains. The tight connection of  $\beta$  sheets immediately transduces the macroscopic chains to a microscopic level. Their results suggested that the mechanical properties of spider silk are closely related to the microscopic pre-strain of amorphous chains. Nova *et al.* (2010) showed that the specific combination of crystalline phase and a semi amorphous matrix is crucial for the unique properties of silk. Their model directly showed that semi-amorphous regions unravel first when silk is being stretched, leading to the large extensibility of silk.

### CONCLUSION

X- ray diffraction pattern of dragline silk of *Nephila pilipes* confirms its semi crystalline nature. This nanostructural features of spider silk plays very important role in enhancing mechanical performance of silk threads. Hence, it can be concluded that this beautiful, naturally golden colored biomaterial having high and stable mechanical performance is found in nature. Successful mass-production of this spider silk with DNA recombinant technology will definitely open a new gate in textile sector.

### ACKNOWLEDGEMENT

Authors are grateful to the Head, Post Graduate Department of Physics, S. G. B. Amravati University, Amravati for providing XRD facility.

### REFERENCES

1. Dionne J, Lefèvre T and Auger M, Major Ampullate Spider Silk with Indistinguishable Spidroin Dope Conformations Leads to Different Fiber Molecular Structures, *Int. J. Mol. Sci.*, 17, 1353, 2016; doi:10.3390/ijms17081353.
2. Du N, Liu XY, Narayanan J, Li L, Lim ML and Li D, Design of superior spider silk: from nanostructure to mechanical properties. *Biophys. J.* 91(12), 2006, pp. 4528-4535.
3. Grubb DT and Jelinsk LW, Fiber morphology of spider silk: the effect of tensile deformation. *Macromolecules*, 30, 1997, pp. 2860-2867.
4. Kennedy CJ, Lerber KV and Wess TJ, Measuring crystallinity of laser cleaned silk by x-ray diffraction. *e-P.S.*, 2, 2005, pp. 31-37.
5. Keten S, Xu Z, Ihle B and Buehler MJ, Nanoconfinement controls stiffness, strength and mechanical toughness of  $\beta$ -sheets crystals in silk, *Nat. Mater.*, 9, 2010, 359-367.
6. Nova A, Ketan S, Pugno N, Redaelli A and Buehler MJ, Molecular and nanostructural mechanisms of deformation, strength and toughness of spider silk fibrils. *Nano Lett.*, 10, 2010, PP. 2626-2634.
7. Papadopoulos P, Solter J and Kremer F, Structure- property relationship in major ampullate spider silk as deduced from polarized FTIR Spectroscopy, *Eur. Phys. J.E.*, 24, 2007, PP.193-199.
8. Riekel C, Bränden C, Craig C, Ferrero C, Heidelbach F and Müller M, Aspects of x-ray diffraction on single spider fibers. *Macromolecules*, 24, 1999, pp. 179-186.
9. Sampath S, Isdebski T, Jenkins JE, Ayon JV, Henning RW, Orgel PRO, Antipoa O and Yarger JL, X-ray diffraction study of nanocrystalline and amorphous structure within major and minor ampullate dragline spider silks. *Soft Matter*, 8(25), 2012, pp. 6713-6722.
10. Sawarkar AS and Sawarkar SB, Spider silk – An ancient material of the future, *IJPRET*, 5 (2), 2016, pp. 236-240.
11. Trancik JE, Czernuszka JT, Bell FI and Viney C, Nanostructural features of a spider dragline silk as revealed by electron and x-ray diffraction studies. *Polymer*, 47, 2006, PP. 5633-5642.